Simultaneous Thermal and Plasma Chemical Activation of Conversions in H_2-I_2-HI Mixtures

Frank Miethke,* Hans-Erich Wagner, Alfred Rutscher, and Siegfried Gundermann

Institute of Physics, Greifswald University, Domstrasse 10a, 17489 Greifswald, FRG

Received: May 12, 1998; In Final Form: August 27, 1998

Chemical quasi-equilibria represent the product composition of stable components at the outlet of a nonisothermal plasma chemical reactor under operating conditions of very high or vanishing electric power input. The properties of these quasi-equilibria in relation to the thermodynamic equilibrium are discussed first of all using an instructive kinetic model. The investigations show that for the formation of the quasi-equilibria the existence of two time scales for the chemical conversions in the system is necessary. The quasi-equilibrium states are formed on a short time scale by fast relaxation and deactivation processes of unstable components. After that the system passes into the thermodynamic equilibrium for very long times. The transition from a chemical quasi-equilibrium state into the thermodynamic equilibrium was detected in the H_2-I_2-HI system experimentally, too. The analysis of a detailed microphysical model for this system shows that the transition into the thermodynamic equilibrium is caused by the increasing thermal production of unstable components (e.g. iodine atoms) at higher gas temperatures. Under these conditions the electronic production of atoms is only a small correction of the thermal degree of dissociation, and the thermodynamic equilibrium is the only stationary state for the system.

Introduction and Motivation

Nonisothermal plasma chemical reactors are systems of high complexity. Examples of these are the different types of gas discharges (glow discharge, microwave discharge, corona discharge, dielectric barrier discharge) operating in reactive gas mixtures. Here the plasma components (electrons, ions, and neutrals) are far from thermodynamic equilibrium. Therefore, the description of chemical reactions requires a detailed kinetic modeling under these conditions (e.g. ref 1). Usually, many of the elementary data (e.g. dependence of electronic cross sections on energy, rate coefficients of radical reactions) are not well-known. To bypass the enormous difficulties of microscopic kinetics, the description of plasma chemical reactions by the methods of statistical physics and thermodynamics has been attempted (e.g. refs 1 and 2). However, this concept is restricted to simple processes. A very useful alternative is the so-called method of macroscopic kinetics.[3,4] This method correlates the chemical conversions in nonisothermal plasma chemical reactors directly to the operation parameters of the reactor (e.g. power input, flow rate). The method allows the calculation of the composition of the stable reaction products at the reactor outlet depending on the reactor operation parameters starting from reversible gross reactions for these components. The essential basis for this concept consists of chemical quasi-equilibrium states reflecting the basic role of reversible gross reactions for the overall behavior of gas discharge reactors. These quasi-equilibria characterize the limit situations of the reactor operation at low power input (in the closed system) and high power input, which includes the limits $n_e \rightarrow 0$ and $n_e \rightarrow \infty$, respectively (n_e is the concentration of plasma electrons). They were qualified as chemical equilibrium of electronic catalysis (CEEC) and chemical equilibrium of complete decomposition (CECD). Various experimental and theoretical investigations in different systems have shown the real existence of these states.[5,6]

In this paper experimental investigations on the formation of chemical quasi-equilibrium states in the model system H_2-I_2-HI as well as on the transition to the thermodynamic equilibrium (TE) are presented. The transition was realized by the common thermal and plasma activation of chemical reactions. The kinetic background is studied in detail on the basis of a microscopic reaction scheme. In a first step the general situation of quasi-equilibrium states and the transition to the thermodynamic equilibrium are analyzed for a simply constructed reaction system containing thermal and electron initiated reactions.

The system H_2-I_2-HI was chosen, because the thermal mechanism of the HI formation is relatively well-known.[7,8] Furthermore, the thermal equilibrium is already arrived at within a moderate reaction time scale ($\tau \leq 10^3$ s) for temperatures below 600 °C. The particle number densities of the stable components n_{H_2}, n_{I_2}, and n_{HI} have the same order of magnitude. After the plasma chemical synthesis of HI, these molecules could be fully decomposed again into H_2 and I_2 by the UV radiation of a mercury lamp. So it was possible to generate a reversible overall chemical process. Therefore, this system is especially suitable for investigating these problems. The main interest was aimed at the question of how the level of the CEEC is influenced by thermally initiated reactions.

Plasma Chemical Quasi-Equilibria

Concept and Definitions. Contrary to the usual chemical equilibrium, the quasi-equilibrium states are related to the special operation conditions of the plasma chemical reactors. It is indispensable to consider the double structure of every plasma chemical reactor, which implies the combination of an active zone with a passive zone in flow systems, separated in space, or an active phase combined with a passive one in closed systems, separated in time.[3] Figure 1 shows the schematic

10.1021/jp982196j CCC: $18.00
Published on Web 03/13/1999

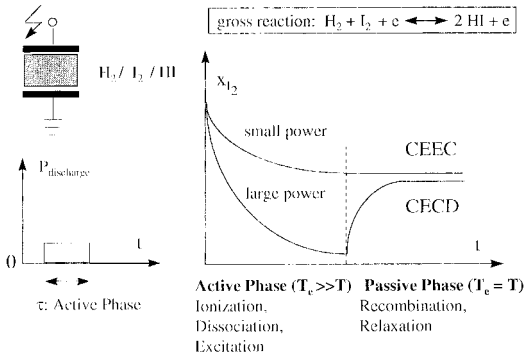

Figure 1. Occurrence of chemical quasi-equilibria in a closed system (illustration for the gross reaction $H_2 + I_2 + e \rightleftharpoons 2HI + e$).

operation of a closed reactor system. During the active phase of the reactor the gas mixture of only stable components is activated by collisions with highly energetic plasma electrons. A variety of reactive unstable components are produced by these processes (radicals, metastable atoms/molecules, ions, etc.). After the discharge interruption the unstable species are deactivated by relaxation and recombination processes. So the gas mixture at the end of a long enough passive phase also contains only stable products, including the input species as well as new components. This product composition which is established after the successive action of both phases in closed systems (at the reactor outlet in flow systems) represents a chemical quasi-equilibrium. Therefore, unstable components are not included. For the limit situation of very high or vanishing electric power input into the active phase (zone) of the reactor the following two quasi-equilibrium states exist:[9]

1. CECD: chemical quasi-equilibrium of complete electronic decomposition. Large concentrations of hot electrons (high power input $P \rightarrow \infty$, followed by $n_e \rightarrow \infty$) result in the nearly complete decomposition of the reactants within the active phase (zone) of the reactor. In the passive phase (zone) the unstable components recombine into stable products, which are detected at the end of the passive phase (zone). This product composition is determined only by the conditions in the passive phase (zone).

2. CEEC: chemical quasi-equilibrium of electronic catalysis. Generally, a finite degree of conversion at the limit of vanishing concentration of hot electrons is produced, representing a kind of electronic catalysis (i.e. $P \rightarrow 0$, $n_e \rightarrow 0$ at $\tau \rightarrow \infty$; τ is the duration time of the active phase (residence time in the active zone)).

Demonstration Example of Chemical Quasi-Equilibria and the Thermodynamic Equilibrium. An instructive model system was analyzed to illustrate the different states of equilibria. The elementary processes are listed in Table 1. The conversion of two species A and B proceeds via "normal" thermal reactions (I) and via excited states marked by an asterisk (II, III, IV). The excited species are produced by collisions with energetic electrons. The rate coefficients were chosen similar to those in the basic mechanism for the ozone synthesis given in ref 3. The numerical computations were performed for a closed system using an explicit Runge−Kutta formalism with step width control.[10] The total particle number density is $n = 3 \times 10^{17}$ cm^{-3}—as is typical for low-pressure gas discharge plasmas. Neglecting thermal reactions (I), the quasi-equilibrium states CEEC and CECD are found at low and high degrees of ionization $x_e = n_e/n$, as shown in Figure 2. The rate coefficients lead to different states CEEC ≠ CECD. Taking into account the thermal reactions, the corresponding thermodynamic equilibrium state predominates at very low x_e. This state will be changed dramatically at higher x_e by the two electronic quasi-

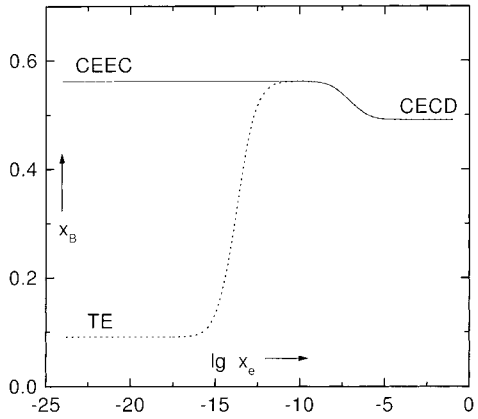

Figure 2. Example of different equilibrium states of the closed reactor for the reaction mechanism given in Table 1 ($k_1 = k_2 = 10^{-10}$ cm^3 s^{-1}, $k_3 = 12$ s^{-1}, $k_4 = 6$ s^{-1}, $k_5 = 10^{-17}$ cm^3 s^{-1}, $k_6 = 10^{-17}$ cm^3 s^{-1}; solid line: $k_+ = k_- = 0$; dashed line: $k_+ = 10^{-7}$ s^{-1}, $k_- = 10^{-6}$ s^{-1}).

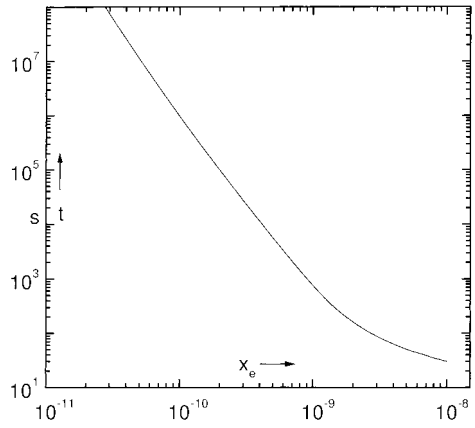

Figure 3. Time required for the formation of the CEEC dependent on the ionization degree (rate constants see Figure 2).

TABLE 1: Demonstration Example

I. thermal reactions	$A \underset{k_-}{\overset{k_+}{\rightleftharpoons}} B$
II. electron-initiated reactions	$A + e \xrightarrow{k_1} A^* + e$
	$B + e \xrightarrow{k_2} B^* + e$
III. modification via excited states	$A^* \xrightarrow{k_3} B$
	$B^* \xrightarrow{k_4} A$
IV. modification via collision processes	$A + B^* \xrightarrow{k_6} B + B^*$
	$A^* + B \xrightarrow{k_5} A^* + A$

equilibrium states. So the transitions from one quasi-equilibrium into the other as well as into the thermodynamic equilibrium are well marked. Especially, it can be seen that the levels of different equilibrium states are independent of x_e. Identical compositions of the stable products are performed starting from both sides of the reversible gross reaction $A + e \rightleftharpoons B + e$. The mole fraction x_B in Figure 2 marks the conditions of the late afterglow but is restricted to times which are small compared with the relaxation time of the thermal reactions ($t \ll \tau_{th} = 1/(k_+ + k_-)$). These dynamic aspects are shown in more detail in Figures 3−5. The time necessary for the formation of the CEEC increases drastically for decreasing ionization degrees, as shown in Figure 3. For ionization degrees $x_e \leq 10^{-11}$ this time is comparable to that required for the formation of the thermodynamic equilibrium. With an x_e smaller than this value the electronic excitation of the gas mixture is a negligible disturbance only. The temporal situation for the formation as

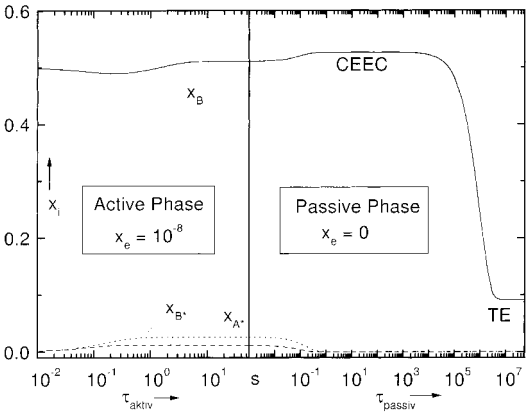

Figure 4. Temporal development of the CEEC as well as the transition into the thermodynamic equilibrium (TE) (input values: $x_{A_0} = x_{B_0} = 0.5$, $x_e = 10^{-8}$).

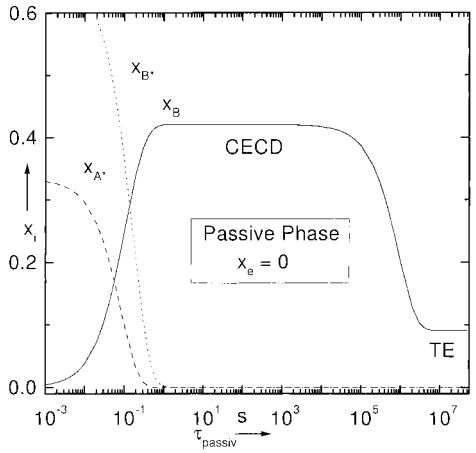

Figure 5. Temporal development of the CECD as well as the transition into the thermodynamic equilibrium (TE) ($x^*_{A_0} = 0.33$, $x^*_{B_0} = 0.66$, $x_e = 0$).

well as the transition from the chemical quasi-equilibrium states into the thermodynamic equilibrium is shown in Figures 4 and 5 for the CEEC and the CECD, respectively. It can be established that the plateaus of the quasi-equilibrium states are formed within a short time after the start of the passive phase. Then the product composition is (nearly) stationary for several orders of magnitude before the system passes into the thermodynamic equilibrium at very large times. This behavior may be understood by discussion of the reaction model given. As one can see, the rate constants for the reactions including the unstable components A* and B* are much greater than k_+ and k_- for the thermal conversions of the products A and B. These conditions are typical of nearly all nonisothermal reactive plasmas. The chemical conversions are initiated by the generation of various very reactive unstable components, which are produced by collision processes of hot plasma electrons with the neutral gas in the active phase. During a short period immediately after the beginning of the passive phase the unstable components generated react into stable products and only for large times does the system pass into the thermodynamic equilibrium caused by the thermally initiated reactions of the stable compounds. For real systems the differences between these two time scales amount to several orders of magnitude. For example, in the case of the H_2-I_2-HI system the CEEC is formed after a few minutes at $T = 300$ K. But the thermodynamic equilibrium would be generated after 10^{10} years under the same conditions.

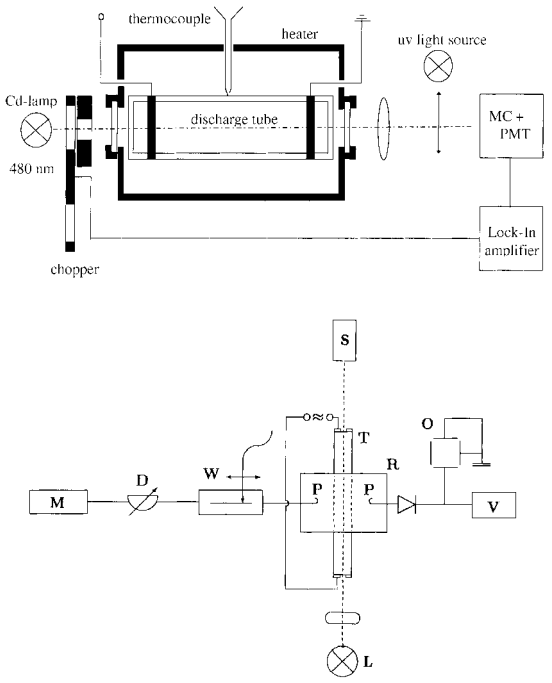

Figure 6. Experimental setup: (top) discharge tube, thermostat and optical components; (bottom) microwave diagnostics device.

To summarize, the chemical quasi-equilibrium states are characterized by the following properties:

1. Quasi-equilibria represent stationary product compositions of only stable compounds after the combined action of the active phase (zone) and the passive phase (zone) of a nonisothermal plasma chemical reactor.

2. They are attainable from both sides of a reversible gross reaction $A + B + e \rightleftharpoons C + e$ of the stable components.

3. The product composition of the quasi-equilibria is independent of the electron concentration (or power input) for several orders of magnitude, the type of plasma zone, or the reactor dead volume.[5]

4. These compositions only depend on the gas temperature. If three-particle collisions are important, the quasi-equilibrium states are influenced by the total particle number density too.[5,6]

A necessary condition for the existence of chemical quasi-equilibrium states consists in the existence of two different time scales for the chemical conversions: on a short time scale the unstable components, generated by electron collision processes in the active phase, recombine in the passive phase into an altered mixture of stable compounds. The transition into the thermodynamic equilibrium follows for large times caused by thermally initiated conversions of the stable products. Therefore, the quasi-equilibria may be interpreted as "kinetic frozen states".

Investigations on the H_2-I_2-HI System

Experimental Setup and Detection Methods. The experimental setup is shown in the parts of Figure 6. The discharges operated in closed quartz tubes T, prepared under high-vacuum conditions. The tubes were filled with well-defined mixtures of iodine and hydrogen (some with admixture of an inert He buffer gas). The discharge tube could be located within a thermostat to perform measurements in the temperature range from 300 to 800 K (Figure 6, top). Vanishing ionization degrees were realized by the excitation of the mixture in a very faint Tesla spark discharge using outer ring electrodes within a tube of 20 mm diameter and 150 mm length. The electric power input was varied, changing the primary voltage of the Tesla

transformer. Higher ionization degrees could be produced in capacitively coupled rf discharges (frequency 450−650 kHz) inside a further tube (diameter 9 mm, length 120 mm). In this case the particle number density of electrons n_e was determined by the microwave cavity method (Figure 6, bottom). The microwave signal from the generator M was coupled into the resonator cavity R by the variable attenuator D, a slotted waveguide W, and the inductive probe P. The adaptation of the resonator to the measuring equipment was checked by the slotted waveguide. The resonator was used as load element and transmission element. The microwave signal, decoupled by the inductive probe, was analyzed by the voltmeter V after its rectification. The oscilloscope O was applied to check the time dependence of the output signal. The interaction of the electric hf field strength E_{hf} with the plasma produces a change Δf of the resonance frequency satisfying the following condition:[11,12]

$$\Delta f = -\frac{2}{3} C \frac{\bar{N}_e}{m_e} e^2 \int_0^\infty \frac{\omega}{\nu^2(U) + \omega^2} U^{3/2} \frac{\partial}{\partial U} (U^{-1/2} F(U))\, dU \quad \text{(i)}$$

where $\bar{N}_e$ is the cross-sectional average value of the electron density; e, and m_e charge and mass of the electron; C geometric factor; $\nu(U)$ electron−neutral particle collision frequency; ω circle frequency of the microwave signal; $F(U)$ energy distribution function of the electrons; U volt equivalent of the electron energy. The geometric factor

$$C = \frac{\int_{V_{pl}} E_{hf}^2\, dV}{\int_{V_r} E_{hf}^2\, dV} \quad \text{(ii)}$$

(where V_{pl} is the plasma volume and V_r the resonator volume) describes the degree of the coupling between the microwave field and the resonator. The distribution function $F(U)$ satisfies the condition

$$\int_0^\infty F(U)\, dU = 1 \quad \text{(iii)}$$

The composition of the stable reaction products was determined by measuring the concentration n_{I_2} of iodine with absorption spectroscopy. The absorption coefficient of I_2 at 480 nm is 1.24×10^{-18} cm^2.[13] Beer's law of absorption was applied. For the experiment a line of 480 nm emitted by Cd lamp L (Figure 6) and detected by the photomultiplier tube S of a monochromator (lock-in technique) was used. The detected I_2 concentration in connection with the filling conditions allowed the particle number densities of H_2 and HI to be calculated in the closed system. After the plasma chemical synthesis of HI, these molecules could be fully decomposed into H_2 and I_2 again by the UV radiation of a mercury lamp.[14,15]

As shown in Figure 7, the spectroscopically determined values of the iodine particle number density are in good agreement with those following from the vapor pressure curve in ref 16, until all I_2 is in the vapor form. Successive runs of the reversible cycle lead to identical values, which represent the initial concentration of I_2. Irreversible processes were not of marked influence inside the discharge tube and therefore the starting conditions could be reproduced.

Results and Discussion

Experimental Investigations. In accordance with the definitions of quasi-equilibrium states presented previously, the formation of a finite conversion in a H_2-I_2 gas mixture at very small ionization degrees takes place, reflecting the formation

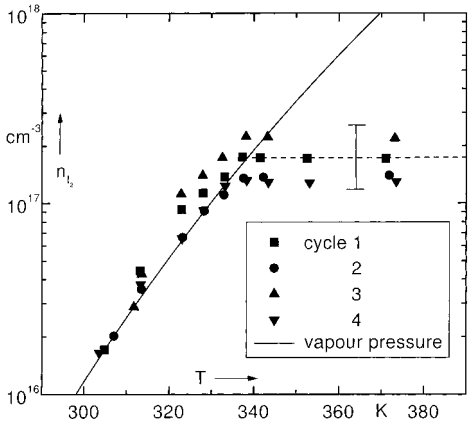

Figure 7. Measured temperature dependence of the iodine concentration in comparison with the vapour pressure curve.[16]

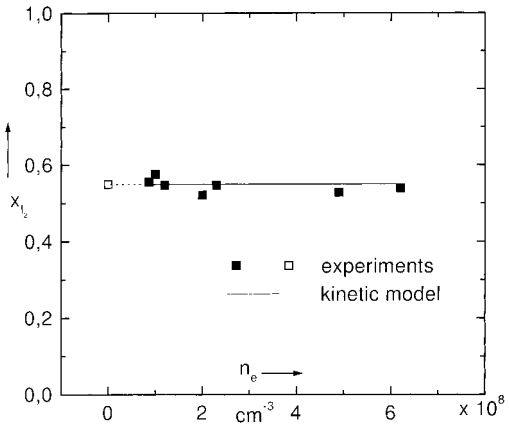

Figure 8. Dependence of the relative iodine concentration on the average concentration of plasma electrons: reactor diameter: 9 mm; length: 120 mm; tube temperature: 360 K; (open square) Tesla spark discharge ($P < 0.1$ W); (filled squares) rf discharge (450−610 kHz); input mixture $x_{I_{2_0}} = 0.61$, $x_{H_{2_0}} = 0.39$; total particle number density: $n = 4.1 \times 10^{16}$ cm^{-3}.

of the CEEC. In Figure 8 the relative I_2 concentration is shown at different, very low, concentrations n_e of plasma electrons in the rf discharge at a constant gas temperature, starting from identical input mixtures (for details see figure legend). Independently of the average ionization degree, an identical composition of the stable reaction products is formed, representing the plateau of the CEEC (Figure 8, full squares). This composition is far from the thermodynamic equilibrium at this temperature. The same composition is produced by the excitation of the mixture in a faint Tesla spark discharge (Figure 8, open square). An example of the temporal development of the CEEC is given in Figure 9, selecting the I_2 component again. A large particle number density of the chemically inert He buffer gas was added to the H_2-I_2 (respectively H_2-I_2-HI) gas mixture. The admixture of He gas enabled the relatively fast generation of the thermodynamic equilibrium at gas temperatures $T \geq 350$ °C, because the time necessary for the formation of this state depends exponentially on the total number density of the process gas.[17] In this way the transition from the CEEC to the thermodynamic equilibrium could be investigated, too. The gas mixture was excited only by the Tesla spark discharge. At a defined gas temperature (here shown for $T = 100$ °C) the reactive mixture changes after a few minutes into the CEEC. Starting from different initial compositions (at a constant total number of H and I atoms) the curves converge into the same quasi-equilibrium state. This result confirms that quasi-equilibria

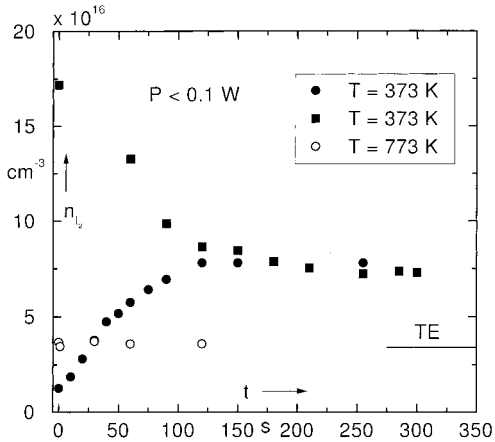

Figure 9. Temporal development of the CEEC (I_2 component) in a Tesla spark discharge at different gas temperatures and initial concentrations: (Full squares) $T = 373$ K, $n_{I_20} = 1.6 \times 10^{17}$ cm^{-3}, $n_{H_20} = 2.1 \times 10^{17}$ cm^{-3}, $n_{HI_0} =$ - cm^{-3}, $n_{He} = 2 \times 10^{19}$ cm^{-3}; (full circles) $T = 373$ K, $n_{I_20} = 2.9 \times 10^{16}$ cm^{-3}, $n_{H_20} = 6.3 \times 10^{16}$ cm^{-3}, $n_{HI_0} = 2.6 \times 10^{17}$ cm^{-3}, $n_{He} = 2 \times 10^{19}$ cm^{-3}; (open circles) $T = 773$ K, $n_{I_20} = 2.9 \times 10^{16}$ cm^{-3}, $n_{H_20} = 6.3 \times 10^{16}$ cm^{-3}, $n_{HI_0} = 2.6 \times 10^{17}$ cm^{-3}, $n_{He} = 2 \times 10^{19}$ cm^{-3}; (line) composition according the thermodynamic equilibrium (TE) for $T = 773$ K.

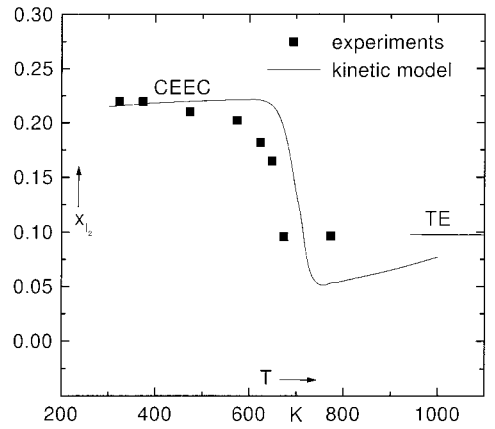

Figure 10. Transition from the CEEC into the thermodynamic equilibrium (TE) at common excitation by a Tesla spark discharge and thermal activation (input mixture as in Figure 9, with $x_{I_2} + x_{H_2} + x_{H_I} = 1$).

are attainable from both sides of the reversible gross reaction $H_2 + I_2 + e \rightleftharpoons 2HI + e$ of the stable components. For a gas temperature of $T = 500$ °C, the thermodynamic equilibrium is fulfilled. Then, in competition between the thermal and discharge excitation, the velocity of the thermal reaction channels dominates. This situation is illustrated in Figure 10 in more detail. At lower temperatures the simultaneous excitation by the spark discharge (with a constant power input) and the thermal activation results in a nearly temperature-independent CEEC. At higher temperatures ($T \geq 350$ °C) the situation is controlled by thermal processes. The kinetic background of these experimental results will be discussed in the next section.

Kinetic Modeling. For a long period the reaction

$$H_2 + I_2 \rightleftharpoons 2HI \qquad (1)$$

was believed to be the prototype for a unimolecular elementary reaction. But Sullivan was able to show by photochemical experiments[7] that the reaction 1 is not an elementary one. On the contrary, reaction 1 is realized by a radical mechanism, including reaction chains of H and I atoms, respectively. This experimental result was confirmed by computations of the collision dynamics of the hydrogen iodine exchange reaction by Sims et al.[8] There it was shown that the reaction

$$HI + HI \rightarrow H_2 + I_2$$

is dynamically forbidden.

TABLE 2: Elementary Processes

species incorporated: e, H, I, I^-, H_2, I_2, HI, H_2I
rate coefficients: k_i in cm^3 s^{-1}, γ_i in cm^6 s^{-1}, α_i in s^{-1}

electronic processes[b]		ref
1.* $H_2 + e \rightarrow H + H + e$	$k_1 = k_1(E/n)(10^{-10})$	25
2.* $I_2 + e \rightarrow I + I^-$	$k_2 = k_2(E/n)(10^{-10})$	24
3.* $HI + e \rightarrow H + I^-$	$k_3 = k_3(E/n)(2 \times 10^{-8})$	23
4. $H_2I + e \rightarrow H_2 + I + I$	$k_4 = k_4(E/n)(10^{-10})$	*a*
5. $I^- + e \rightarrow I + e + e$	$k_5 = k_5(E/n)(10^{-8})$	*a*
5a. $I^- + M^+ \rightarrow I + M$	$k_{5a} = k_{5a}(E/n)(10^{-7})$	*a*
thermal processes[b]		**ref**
6. $I^- + M \rightarrow I + M + e$	$k_6 = 10^{-14}$	*a*
7. $I + I^- + M \rightarrow I_2 + M + e$	$\gamma_7 = 2.3 \times 10^{-30}$ (M = I_2)	*a*
8.* $I + \text{wall} \rightarrow {}^1/_2I_2$	$\alpha_8 = \epsilon\bar{v}_I/(2r_0)$, $\epsilon = 10^{-4}$	*a*
9.* $H + \text{wall} \rightarrow {}^1/_2H_2$	$\alpha_9 = \epsilon\bar{v}_H/(2r_0)$, $\epsilon = 10^{-4}$	26
10.* $HI + I \underset{k_{-10}}{\overset{k_{10}}{\rightleftharpoons}} H + I_2$	$k_{10} = 9.1 \times 10^{-9}T^{0.5}e^{-18041/T}$ $k_{-10} = 6.6 \times 10^{-10}e^{-20/T}$	21, 22
11.* $HI + H \underset{k_{-11}}{\overset{k_{11}}{\rightleftharpoons}} I + H_2$	$k_{11} = 7.4 \times 10^{-11}e^{-290/T}$ $k_{-11} = 5.9 \times 10^{-9}T^{0.5}e^{-16529/T}$	21, 22
12. $I + I + H_2 \underset{k_{-12}}{\overset{\gamma_{12}}{\rightleftharpoons}} H_2I + I$	$\gamma_{12} = 1.3 \times 10^{-32}$ $k_{-12} = 4.3 \times 10^{-10}$	8
13. $H_2I + I \rightarrow 2HI$	$k_{13} = 8.8 \times 10^{-14}$	8
14. $I_2 + M \underset{\gamma_{-14}}{\overset{k_{14}}{\rightleftharpoons}} I + I + M$	$k_{14} = 5.3 \times 10^{-4}T^{-1.8}e^{-17910/T}$ $\gamma_{-14} = 2.3 \times 10^{-30}$ (M = I_2)	21
15. $H_2 + M \underset{\gamma_{-15}}{\overset{k_{15}}{\rightleftharpoons}} H + H + M$	$k_{15} = 2.9 \times 10^{-4}T^{-1.5}e^{-52007/T}$ $\gamma_{-15} = 3 \times 10^{-32}$	21

[a] Adapted. [b] M = He if not specified.

The Studied Reaction Mechanism. To understand the background of the formation of chemical quasi-equilibrium states as well as the transition to the thermal equilibrium, a kinetic model was developed. The reaction channels considered and the types of particles incorporated (electrons e, neutral atoms H, I, molecules H_2, I_2, HI, reactive intermediates H_2I, and negative iodine ions I^-) are summarized in Table 2. The coefficients used for the electronic collision processes are given in parentheses. The helium atoms were considered to act only as inert collision bodies for the thermal dissociation of I_2 and H_2 as well as for the recombination of I and H atoms by three-particle collisions. These processes do not have marked influence on the equilibrium composition. So for these reactions in each case identical rate coefficients were used. If M is not specified, the rate coefficient is given for M = He. The neutralization process of the negative iodine ions I^- (channel 5a) was taken into account to ensure the required quasi-neutrality of the plasma. The concentration of the positive ions is nearly that of the negative ions, caused by the very strong electronegativity of the H_2-I_2-HI system. The numerical computations were performed using the program package CHEMKIN[18] for a closed system with constant gas temperature as well as constant total particle number density. All numerical results refer to idealized discharge conditions (no intermittances; continuous and homogeneous active phase). But the equilibrium values should be correct also for the intermittent Tesla discharge because of the great chemical time constants. The same is suitable for small times ($\tau \leq 10^{-3}$ s) as shown e.g. in ref 19. The thermodynamic data for the compounds including iodine were taken from ref 20.

At first it was verified that the mechanism used is suitable to calculate the thermodynamic equilibrium. In Figure 11 the

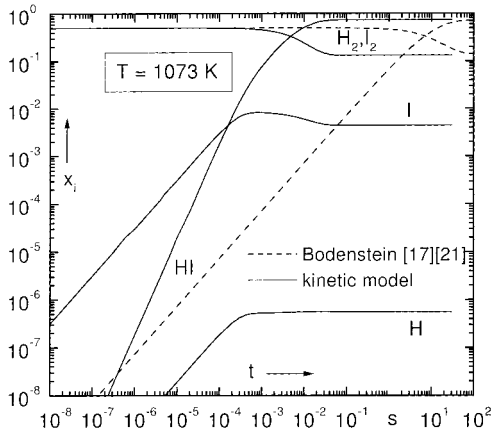

Figure 11. Temporal development of the product composition of the thermodynamic equilibrium calculated by the kinetic model (see Table 2) as well as by the gross reaction 1.[17]

numerical results, according to the thermal reactions of the mechanism given in Table 2, are compared with the product composition calculated by the gross equation 1 according to ref 17. The rate coefficients for (1) are given in ref 21. Both computations excellently describe the product composition of the thermodynamic equilibrium, but they differ in the time dependence. This result is in accordance with that of Sims et al.[8] These authors showed in detail that reaction 1 is not suitable to describe the dynamical behavior of the H_2-I_2-HI system. Furthermore the kinetic model describes in a sufficient manner the experimentally detected—n_e independent—plateau of the CEEC (see Figure 8). The detailed analytical analysis of the system of balance equations for the proposed reaction mechanism showed that the composition of the CEEC is estimated by a small number of elementary processes, which are marked by a * in Table 2. It can be emphasized that at the extreme situation of the CEEC (i.e., $n_e \rightarrow 0$) all those reaction channels have no influence which are of second order regarding the unstable intermediate species. Within a factor of 2 the CEEC can be calculated by the following simple relation

$$\frac{x^0_{H_2}\, x^0_{I_2}}{x^{02}_{HI}} \approx 0.5\, \frac{k_3\, k_{11}}{k_1\, k_{-10}}$$

where the superscript zero denotes the case $n_e \rightarrow 0$.

Surprisingly, the formula has the form of a mass action law. This formula shows that the CEEC is fixed by reaction channels generating or consuming H atoms. In contrast to this situation the thermal HI formation is dominated by I atoms (channels 14, −11, 12, 13). This will be discussed below.

Interpretation of the Experimental Results by the Kinetic Model. As shown in Figure 10, the model calculations are in good agreement with the experimental results for the dependence of the CEEC on the gas temperature, too. At lower values ($T <$ 600 K) the common excitation results in a nearly temperature-independent CEEC. To the right of a sharp transition region (600 K $< T <$ 680 K) the product composition detected is controlled by the thermodynamic equilibrium. At these temperatures the weak excitation by electronic processes is not able to alter the gas composition. The explanation for this behavior can be taken from Figure 12a and Figure 12b. There the calculated dependences of the concentrations of the H and the I atoms on the gas temperature are plotted for different ionization degrees x_e. For low gas temperatures the dissociation into atoms is determined only by the electronic processes (reactions 1 and 2 in Table 2). For increasing temperatures the importance of the thermal dissociation processes (reactions 14 and 15 in Table 2) increases in relation to the electronic ones. Therefore, at high gas temperatures the thermal dissociation dominates the creation of the iodine atoms. Then the electronic excitation of the gas mixture is only a small disturbance of the system. Under these conditions the chemical quasi-equilibrium states do not exist

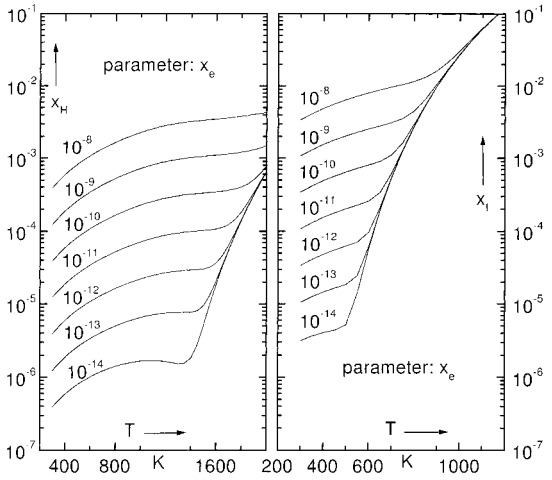

Figure 12. Temperature dependence of the relative concentration of the H atoms (a, left) and I atoms (b, right) at various ionization degress.

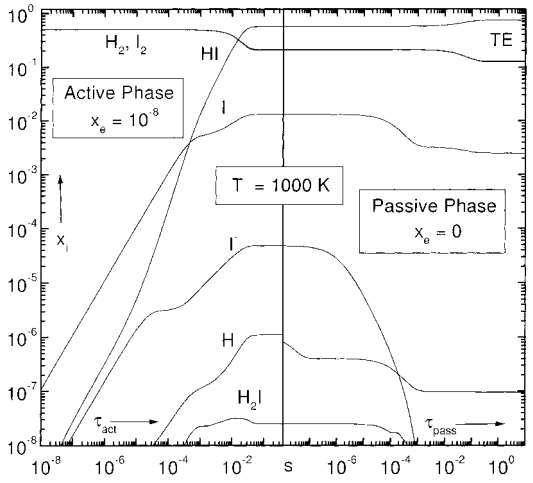

Figure 13. Temporal development of the gas composition at $T = 1000$ K for a stoichiometric input mixture ($x_{I_20} = x_{H_20} = 0.5$).

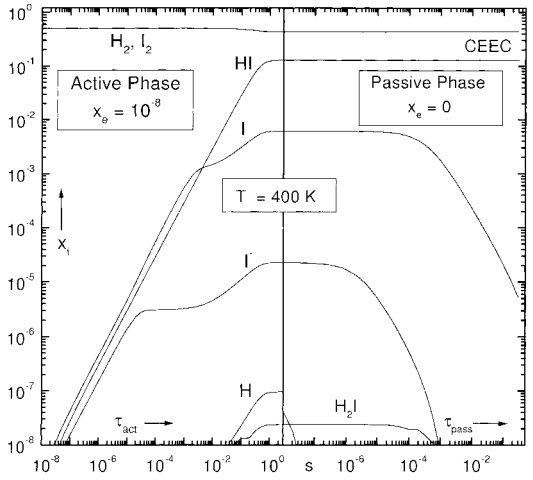

Figure 14. Temporal development of the gas composition at $T = 400$ K for a stoichiometric input mixture ($x_{I_20} = x_{H_20} = 0.5$).

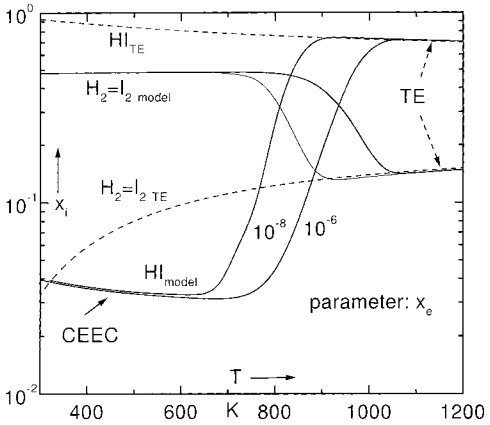

Figure 15. Calculated composition of the stable reaction products on the gas mixture according the kinetic model (for $x_e = 10^{-6}$, $x_e = 10^{-8}$, $n_0 = 3 \times 10^{17}$ cm^{-3}, ($x_{I_{20}} = x_{H_{20}} = 0.5$).

and the thermodynamic equilibrium is the only stationary state of the gas mixture. The time dependence of the formation of the thermodynamic equilibrium is illustrated in Figure 13 for a stoichiometric input mixture at $T = 1000$ K. The electronic excitation of the input mixture in the active phase as well as the relaxation of the system in the passive phase are shown. This relaxation is subdivided into two steps. The first step is characterized by the recombination of the unstable hydrogen atoms as well as of the ionic component ($\tau_{pass} \leq 10^{-3}$ s). But the concentration of the thermally produced iodine atoms is relatively high at this gas temperature. Therefore, these atoms cause the second step, which leads to the formation of the thermodynamic equilibrium after about 1 s. In contrast to this, the second step cannot be seen at lower gas temperatures. One example is given in Figure 14 illustrating this situation for the same input mixture at $T = 400$ K. The transition from the CEEC to the thermodynamic equilibrium at common plasma and thermal excitation dependent on the gas temperature is summarized in Figure 15 for all stable components of a stoichiometric mixture. Additionally, the product composition is shown at pure thermal activation. Depending on the ionization degree, the transition is shifted to lower or higher temperatures, here plotted for two typical x_e values. The curves converge at low and at high temperatures into quite different levels of the product composition, which are, however, independent of the ionization degrees. These results stress the given definition of the CEEC as well as the dominance of thermal reactions at high temperatures, creating the distribution of the thermodynamic equilibrium.

Acknowledgment. The work was supported by the "Deutsche Forschungsgemeinschaft", Sonderforschungsbereich 198 "Kinetics of partially ionized plasmas".

References and Notes

(1) Veprek, S. *Chimia* **1980**, *34* (12), 489.

(2) Veprek, S. *J. Chem. Phys.* **1972**, *57* (2), 952.

(3) Rutscher, A.; Wagner, H.-E. *Contr. Plasma Phys.* **1985**, *25* (4), 337 Rutscher, A., Wagner, H.-E. *Inv. Paper, ICPIG 18 (Swansea, Wales)* **1987**, 172.

(4) Eremin, E. N. *Elementy gazovoi electrochimii*; Moskva, 1968.

(5) Rutscher, A.; Wagner, H.-E.; Lucke, W.; Miethke, F. *Proc. ISPC 11 (Loughborough, England)* **1993**, 1356.

(6) Miethke, F.; Rutscher, A.; Wagner, H.-E. *Proc. ICPIG 21 (Bochum, FRG)* **1993**, 205.

(7) Sullivan, J. H. *J. Chem. Phys.* **1967**, *46* (1), 73.

(8) Sims, L. B.; Porter, R. N.; Raff, L. M.; Thompson, D. L. *J. Chem. Phys.* **1972**, *56* (12), 5998.

(9) Rutscher, A.; Wagner, H.-E. *Plasma Sources Sci. Technol.* **1993**, *2*, 279.

(10) Reuter, F.; Engeln-Müllges, G. *Formelsammlung zur Numerischen Mathematik mit Turbo Pasacal—Programmen*; BI Wissenschaftsverlag: Vienna, 1991.

(11) Slater, J. C. *Rev. Mod. Phys.* **1946**, *18*, 473.

(12) Gundermann, S.; Winkler, R. *Beitr. Plasmaphys.* **1975**, *15*, 251.

(13) Tellinghuisen, J. *J. Chem. Phys.* **1973**, *58* (7), 2821.

(14) Xu, Z.; Koplitz, B.; Wittig, C. *J. Chem. Phys.* **1989**, *90* (5), 2962.

(15) Brewer, P.; Das, P.; Ondrey, G.; Bersohn, R. *J. Chem. Phys.* **1983**, *79* (2), 720.

(16) Landolt-Börnstein *Zahlenwerte und Funktionen*, Springer-Verlag: Berlin, 1960; Vol. II, 2. Teil, Bandteil a.

(17) Bodenstein, M. *Z. Phys. Chem.* **1899**, *29*, 295.

(18) National Laboratories, Thermal and Plasma Processes Department, Livermore, CA 94551−0969.

(19) Eliasson, B.; Simon, F. G.; Egli, W. *Non-Thermal Plasma Techniques for Pollution Control*; NATO ASI Series, Vol. G 34, Part B; Penetrante, B. M., Schultheis, S. E., Eds.; Springer-Verlag: Berlin, 1993.

(20) Leonidov, W. Ja.; Gurvitsch, L. W.; Iorisch, W. S. *Termodinamitscheskije swoistwa individualnych weschtschestw*, Isdatelstvo "Nauka": Moscow, 1978; Vol. 1, No. 2.

(21) *Landolt-Börnstein Zahlenwerte und Funktionen*, Springer-Verlag: Berlin, 1968; Vol. II, 5. Teil, Bandteil b.

(22) Lorenz, K.; Wagner, H. Gg.; Zellner, R. *Ber. Bunsen-Ges. Phys. Chem.* **1979**, *83*, 556.

(23) Smith, D.; Adams, N. G. *J. Phys. B: At. Mol. Phys.* **1987**, *20*, 4903.

(24) Ayala, J. A.; Wentworth, W. E.; Chen, E. C. M. *J. Phys. Chem.* **1981**, *85*, 768.

(25) Janev, R. K.; Langer, W. D.; Evans, K., Jr.; Post, J. E. Jr. *Elementary Processes in Hydrogen−Helium Plasmas*; Springer-Verlag: Berlin, 1987.

(26) Venugopalan, M.; Jones, R. A. *Chemistry of Dissociated Water Vapour and Related Systems*; Interscience Publisher: New York, 1968.